Acta Biomaterialia 6 (2010) 2477–2483

Contents lists available at ScienceDirect

Acta Biomaterialia

journal homepage: www.elsevier.com/locate/actabiomat

A facile method to fabricate poly(L-lactide) nano-fibrous morphologies by phase inversion

Bernke J. Papenburg [a], Lydia A.M. Bolhuis-Versteeg [a], Dirk W. Grijpma [b,c], Jan Feijen [b], Matthias Wessling [a], Dimitrios Stamatialis [a,*]

[a] Membrane Science and Technology, Faculty of Science and Technology, MIRA Institute for BioMedical Technology and Technical Medicine, University of Twente, P.O. Box 217, 7500 AE, Enschede, The Netherlands
[b] Polymer Chemistry and Biomaterials, Faculty of Science and Technology, MIRA Institute for BioMedical Technology and Technical Medicine, University of Twente, P.O. Box 217, 7500 AE, Enschede, The Netherlands
[c] Department of Biomedical Engineering, University Medical Center Groningen, University of Groningen, Antonius Deusinglaan 1, 9713 AV, Groningen, The Netherlands

ARTICLE INFO

Article history:
Received 10 August 2009
Received in revised form 21 December 2009
Accepted 29 December 2009
Available online 4 January 2010

Keywords:
Poly(L-lactic acid)
Phase separation
Molecular weight
Porosity
Nano-fiber

ABSTRACT

Scaffolds with a nano-fibrous morphology are favored for certain tissue engineering applications as this morphology mimics the tissue's natural extracellular matrix secreted by the cells, which consists of mainly collagen fibers with diameters ranging from 50 to 400 nm. Porous poly(L-lactide) (PLLA) scaffolds obtained by phase inversion methods generally have a solid-wall pore morphology. In contrast, this work presents a facile method to fabricate highly porous and highly interconnected nano-fibrous scaffold sheets by phase inversion using PLLA of very high molecular weight (5.7×10^5 g mol^{-1}). The scaffold sheets consist of nano-fibers within the desired range of 50–500 nm. When applying phase separation micromolding as a fabrication method besides the porous nano-fibrous morphology, an additional topography can be introduced into these sheets. Culturing of C2C12 pre-myoblasts on these nano-fibrous sheets reveals very good cell adhesion, morphology and proliferation. Excellent alignment of the cells is induced by fabrication of 25 μm wide microchannels in these sheets. These results warrant further evaluation of these sheets as tissue engineering scaffolds.

1. Introduction

In tissue engineering (TE), many methods are applied to design and manufacture porous scaffolds as carriers for cell growth. Several common fabrication methods are based on phase separation including liquid-induced phase separation (LIPS, immersion precipitation) or thermally induced phase separation (TIPS) [1,2]. The obtained morphology as well as the corresponding feature sizes may vary widely depending on the processing conditions; from dense to highly porous, with pores from sub-micron scale to tens of microns and from non-percolated to highly interconnected. There are also many literature reports on scaffold fabrication using the well-known biopolymer poly(L-lactic acid) (PLLA) via LIPS [3–6] or TIPS [7–9]. In most of these studies, the resulting porous sheets comprise generally of non-percolated pore morphology distinguished by rather rounded pores (solid-wall pore morphology).

In certain tissue engineering applications, however, fibrous morphologies are favored over solid-wall pore morphologies as the nano-fibers resemble the natural environment that surrounds the cells [10–14]. Collagen fibers, which make up the main component of the extracellular matrix (ECM) secreted by cells, have fiber diameters ranging from 50 to 400 nm [11]. In fact, improved cell adherence, proliferation, migration and differentiation have been observed for various cell types on nano-fibrous scaffolds, independently of the fabrication method [15]. These studies report increased protein adsorption to the nano-fibrous scaffolds leading to increased cell attachment, which is important for most cell types to proliferate, migrate and differentiate [15]. To prepare sheets with a nano-fibrous morphology, electrospinning is the most common fabrication method. Variation of the electrospinning process conditions enables e.g. tuning fiber dimensions generally within a range of around 100 nm to 100 μm or more [16–19]. Recently, some literature reports appeared on the formation of nano-fibrous porous sheets by LIPS [20,21]. However, the reported protocols require thermal quenching steps and are relatively time-consuming and elaborate processes.

In this work, we present a facile method to fabricate highly porous nano-fibrous sheets via LIPS, in contrast to the generally obtained solid-wall-like pore morphology in the micrometer-size range [3], through increasing the molecular weight of the PLLA. The dimensions of the obtained nano-fibers range between 50 and 500 nm. In addition, by using phase separation micromolding

* Corresponding author. Tel.: +31 53 4894675; fax: +31 53 4894611.
E-mail address: d.stamatialis@utwente.nl (D. Stamatialis).

1742-7061/$ - see front matter © 2009 Acta Materialia Inc. Published by Elsevier Ltd. All rights reserved.
doi:10.1016/j.actbio.2009.12.051

(PSμM), a micropattern can be included into these nano-fibrous sheets. With PSμM, casting of the polymer solution occurs on a micropatterned mold, enabling replication of the inverse micropattern into a polymer sheet during solidification. Micropatterning of the scaffold surface is known to assist cell organization and to promote functionality of the cells or tissue [3,22]. The effect of polymer concentration, initial casting thickness as well as micropattern replication onto the final nano-fibrous morphologies is discussed and compared to PLLA sheets comprising solid-wall pore morphology with micrometer-size pores. In addition, C2C12 pre-myoblasts are cultured to evaluate cell adhesion, spreading and alignment on these nano-fibrous sheets.

2. Materials and methods

2.1. PLLA synthesis and characterization

High-molecular-weight poly(L-lactide) (PLLA) and very-high-molecular-weight PLLA were prepared on a 100 g scale by ring opening polymerization of L-lactide (Purac Biochem) under vacuum in a heat-sealed glass ampoule. The polymerization was conducted at 130 ± 1 °C for 3 days using stannous octoate (2×10^{-4} mol per mol L-lactide) as catalyst. The polymer was purified by dissolution in chloroform, precipitated into an excess of ethanol and subsequently dried in vacuo at room temperature.

The number average (M_n) and weight average (M_w) molecular weights, molecular weight distribution (M_w/M_n) and intrinsic viscosity ([η], in chloroform) of the polymer were determined by gel permeation chromatography (GPC) using chloroform as eluent at 30 °C. The GPC setup (Viscotec) consisted of a GPCmax VE-2001 GPC solvent/sample module, a series of ViscoGEL I columns, and a TDA 302 triple detector array comprising a light scattering detector, a differential refractive index detector and a four-capillary differential viscometer.

The peak melting temperature (T_m) and the glass transition temperature (T_g) of the polymer were determined by differential scanning calorimetry (Pyris 1 DSC, Perkin Elmer) at a heating rate of 10 °C per min. Indium and gallium were used as standards for temperature calibration. The peak melting temperature was determined from the first heating scan (up to 225 °C). The glass transition temperature was determined after quenching to −80 °C in a second scan. The glass transition temperature was taken as the midpoint of the heat capacity change.

2.2. Scaffold preparation and characterization

Precipitated very-high-molecular-weight PLLA, from this point on referred to as "PLLA HMw", was dissolved in 1,4-dioxane at concentrations of 0.5–2 wt.% and ethanol was used as nonsolvent at 2–4 °C (both Merck, analytical quality). The sheets were cast at initial casting thicknesses between 150 and 1000 μm and immediately after casting they were submerged into the nonsolvent to induce phase separation. After a couple of minutes, the sheets released from the molds were left in the nonsolvent for 18–24 h and subsequently washed thoroughly in Milli-Q water for 4–8 h to ensure removal of the residual solvent and nonsolvent. Finally, the sheets were dried in a controlled atmosphere (T = 19–21 °C). All procedures were performed at room temperature (T = 19–21 °C) unless stated otherwise.

As control, high-molecular-weight PLLA with $M_w = 1.6 \times 10^5$ g mol^{-1} and $M_n = 8.4 \times 10^4$ g mol^{-1} was used as well, from this point on referred to as "PLLA control". PLLA control was dissolved in 1,4-dioxane at a 5 wt.% concentration and was cast at an initial casting thickness of 150 μm (nonpatterned mold) or 200 μm (patterned mold). Further, the casting, phase separation, washing and drying parameters were similar to the PLLA HMw sheets.

For the cell culturing experiments, circular samples of 15 mm were cut from the sheets, and immersed in a 70% ethanol solution for 20–30 min, followed by evaporation of the ethanol in the air. The samples were placed in 24-well plates (tissue culture treated surface, Nunc) and an o-ring (Viton type 51414, 14x1, Eriks) of the exact inner diameter of the well was placed on top to prevent floating of the samples. The samples were sprayed with 70% isopropanol solution and placed in a laminar flow cabinet to allow isopropanol evaporation. The sheets were finally washed and stored for at least 24 h in PBS at 37 °C in a humid atmosphere with 5% CO_2 to ensure complete wetting.

Sheets with and without a pattern were prepared. The nonpatterned sheets, indicated with "np", were cast on flat molds where the patterned sheets were cast on molds featuring 25 μm wide channels and are indicated with "25 μm" (channel width = 25 μm, ridge width = 25 μm, channel height = 30 μm). Besides, the "air side" of the sheets indicates the top side of the scaffold during casting, where the "substrate side" indicates the side in contact with the mold during casting, i.e. the possibly patterned side.

Scanning electron microscopy (SEM, JEOL 5600LV) was applied for the primary characterization of the sheet morphology. For this, the samples were sputter-coated with a nm-thick gold layer prior to imaging. The sheet thickness was determined from these images and was used to calculate the overall porosity by volume, weight and density (a method described in detail elsewhere [3]).

2.3. Cell culture and analysis

Morphology of pre-myoblasts, C2C12, on the PLLA scaffolds was visualized by fluorescence microscopy and SEM to evaluate cell behavior.

2.3.1. Culturing

C2C12 cells were cultured in proliferation medium containing Dulbecco's Modified Eagle's Medium (D-MEM, Gibco) supplemented with 10% fetal bovine serum (FBS, Cambrex), 100 U ml^{-1} penicillin (Gibco) and 100 μg ml^{-1} streptomycin (Gibco) at 37 °C in a humid atmosphere with 5% CO_2. In the expansion phase, the cells were plated at 2000–3000 cells cm^{-2} and upon reaching 70–80% confluency detached by trypsination (0.05% trypsin containing 1 mM EDTA) and subsequently sub-cultured or seeded on the PLLA sheets at a seeding density of 5000–15,000 cells cm^{-2}. The medium was refreshed every other day. Cell numbers were determined by manual counting with a haemacytometer. To prevent confluence and therefore to enable the visualization of single cells, the culturing period was only up to 4 days. Culturing experiments were performed in duplicate for every type of scaffold sheet including the air side, as well as the substrate side, of the sheets.

2.3.2. Fixation and staining for fluorescence microscopy

At day 3, the medium was aspirated from the wells, the sheets were washed with PBS, fixated by incubation with 4%-paraformaldehyde (Merck) in PBS for 30–60 min, and again washed with PBS. To stain the cells, PBS was aspirated and the cells were permeabilized by a 0.1% Triton-X100 solution for 2–3 min and washed twice with PBS. Subsequently, the cells were incubated for 10–15 min with the staining solution containing 2.5 vol.% AlexaFluor 488 phalloidin and 0.1 vol.% Hoechst (both Invitrogen) in PBS to stain the cytoskeleton (F-actin) and nucleus, respectively. Finally, the sheets were washed and stored in PBS and placed at 4 °C upon imaging (within 1 week) by fluorescence microscopy (BD Pathway 435, BD Biosciences).

2.3.3. SEM imaging

SEM imaging was performed on the same samples after fluorescence microscopy. PBS was aspirated and the sheets were washed twice with water to ensure full removal of all salts. Subsequently, the sheets were dehydrated using a water-to-ethanol gradient (ratios water:ethanol 100:0, 50:50, 25:75, 10:90, 5:95, and 0:100) and finally dried in air at room temperature. Finally, the samples were kept under vacuum at 30 °C to ensure complete drying and the nm-thick gold coating was applied.

2.3.4. Proliferation assay

As measure for cell proliferation total DNA was determined per sheet, performed in biological triplicates. After aspirating the medium from the wells, the sheets were washed with PBS and subsequently the cells were lysed (cell culture lysis reagent part #E153A, Promega). DNA concentration per sheet was determined using a cell proliferation assay following the manufacturer's protocol (CyQuant Cell Proliferation Assay Kit, Invitrogen/Molecular Probes). Statistical significance was calculated using the two-tailed *t*-test at $p < 0.05$.

3. Results and discussion

3.1. PLLA synthesis and characterization

High-molecular-weight PLLA was synthesized with M_w of 5.72×10^5 g mol^{-1}, M_n of 4.33×10^5 g mol^{-1} and a molecular weight distribution (M_w/M_n) of 1.32. The intrinsic viscosity [η], using chloroform, was 6.69 dl g^{-1}. The semicrystalline polymer has a glass transition temperature of 60 °C, a melting temperature of 179.4 °C and a heat of fusion of 40 J g^{-1}.

3.2. Scaffold preparation

During phase separation, demixing results in two phases: a polymer-rich phase and a solvent-rich (or polymer-lean) phase. One phase forms the continuous phase and the second phase forms the dispersed phase. At very low polymer concentrations, the solvent-rich phase forms the continuous phase with a dispersed polymer-rich phase. As the concentration increases reaching the critical polymer concentration, the polymer-rich phase becomes the continuous phase instead resulting in a polymer matrix with pores evolving from the dispersed solvent-rich phase.

Initially in this study, low concentrations of PLLA HMw were used for sheet formation. With polymer solutions of 0.5 and 0.75 wt.% in dioxane, no sheet formation occurs for initial casting thicknesses up to 500 μm. Presumably, these concentrations are below the critical polymer concentration necessary to obtain a continuous polymer matrix. However, a 1 wt.% PLLA HMw solution cast with an initial thickness of 400 μm results in the formation of a thin sheet. Therefore, 1 wt.% is considered as a concentration equal to or above the critical polymer concentration for this system. For a 1.25 wt.% polymer solution, sheet formation occurs at initial casting thicknesses of 150 μm or more, although the mechanical strength of the sheets is only acceptable for an initial casting thickness of 350 μm or more. Polymer concentrations of 1.5 and 2 wt.% cast at 150 μm or thicker result in the formation of good quality, well manageable sheets. The viscosity of the 2 wt.% polymer solution is rather high and casting is not practical, and therefore 2 wt.% was the upper limit used in this study. Based on the above results, PLLA HMw-dioxane solutions of 1, 1.5 and 2 wt.% were selected for further sheet fabrication with initial casting thicknesses of 500 and 1000 μm.

3.3. Scaffold characterization

In previous work, PLLA control ($M_w = 1.6 \times 10^5$ g mol^{-1}, $M_n = 8.4 \times 10^4$ g mol^{-1}) was used to fabricate micropatterned sheets with a solid-wall-like pore morphology by PSμM [3]. There, the critical polymer concentration was 5 wt.% for all casting thicknesses [3]. Application of PLLA HMw allows using solutions with lower polymer concentrations for achieving sheet formation. Interestingly, under similar processing conditions, the PLLA HMw used in this work leads to nano-fibrous morphologies. Fig. 1 compares SEM images of sheets cast from PLLA HMw and PLLA control sheets and reveals large differences in sheet morphology of the two cases. Clearly, both PLLA HMw and PLLA control sheets are moderately to highly porous and interconnected; however, the PLLA HMw sheets consist of nano-fibers with diameters in the range of 50–500 nm in contrast to the micrometer-size solid-wall pore morphology of PLLA control sheets. In general, the majority of the fibers at the inner part of the PLLA HMw sheets have a diameter of 50–200 nm and at the surfaces of 100–300 nm. For the nano-fibrous PLLA HMw sheets, the pore connectivity is very high, as indicated by the high transport of fluids through the sheets during handling steps and of culture medium during cell culture. In fact, the diffusivity of glucose through these sheets is similar to glucose diffusion in the medium. In contrast, the diffusivity of glucose through the PLLA control sheets is almost an order of magnitude lower than the free diffusion of glucose [3].

From this data, it is obvious that the molecular weight of the polymer influences the obtained morphology and can be related to fundamental aspects of phase separation. It is well known in polymer science [23–28] that in solution the stability of a transient network is related to the number of entanglements per polymer chain. In solution, the molecular weight between entanglements ($M_{\varepsilon,sol}$) is related to the volume fraction of the polymer ϕ through Eq. (1):

$$M_{\varepsilon,sol} = M_{\varepsilon,melt}\, \phi^{-\alpha} \quad (1)$$

where $M_{\varepsilon,melt}$ represents the molecular weight between entanglements in the undiluted polymer and α is a constant in the range between 1.0 and 1.3. Obviously, at a given polymer concentration (wt.%), the higher the molecular weight of the polymer is, the higher the number of entanglements per chain will be, and the more stable the transient network will be during the phase separation process. This dilute and stable network will be able to phase-separate into a solid, nanostructured polymer morphology. In fact, at the critical overlap concentration of a polymer in solution, the molecular chains start to overlap with each other, resulting in the formation of intermolecular entanglements. At a given polymer concentration (expressed as wt.% or vol.%) above the critical overlap concentration, the molecular weight between these entanglements is constant. As a result, the number of entanglements per polymer chain is therefore higher for polymer chains of higher molecular weight. Furthermore, their relaxation times are longer as well. The increased number of entanglements per polymer chain for the higher-molecular-weight polymer, combined with the longer relaxation times, lead to an increased strength of the transient network.

During the phase separation process, mixing of the solvent with the nonsolvent will reduce the solvent quality and induces the PLLA-rich phase to crystallize and solidify [29]. Early in the phase separation process as well as with very low polymer concentrations, the polymer-rich phase characteristic sizes are still very small. In the case of PLLA HMw, the increased network strength allows for the formation of a continuous nucleated polymer phase at very low polymer concentrations (i.e. critical polymer concentration). In the case of the control (low M_w) PLLA, the transient network is not strong enough to support the polymer-rich phase to

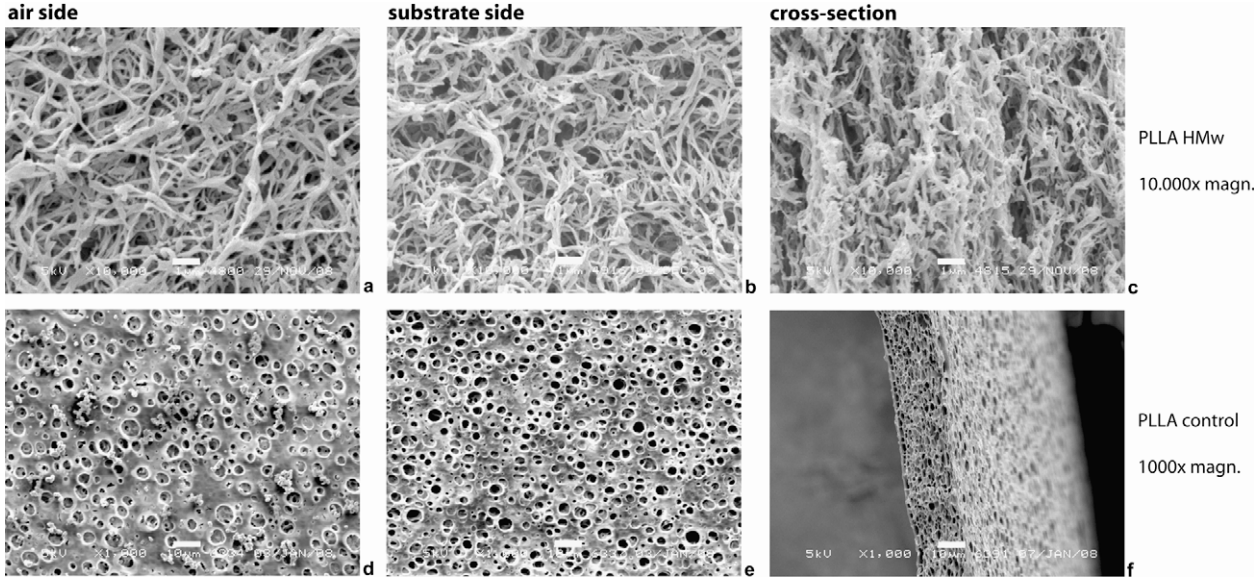

Fig. 1. Typical SEM images of nonpatterned sheets cast of (a–c) 2 wt.% high-molecular-weight PLLA (PLLA HMw) solution and (d–f) a 5 wt.% control PLLA solution; (a, d) air side, (b, e) substrate side, (c, f) cross-section. Scale bar in images represents (a–c) 1 μm and (d–f) 10 μm.

form the continuous matrix at such a low polymer concentration, and will stay as the dispersed phase instead. As a result, the PLLA HMw sheets can be formed at much lower polymer concentrations and the resulting characteristic sizes are smaller, in this case leading to the formation of these nano-sized fiber structures.

3.4. Effect of PLLA HMw concentration and initial casting thickness

Besides the polymer concentration, the initial casting thickness influences the final sheet morphology. In general, increasing the initial casting thickness from 500 to 1000 μm leads to thicker sheets. In contrast, for the sheets cast from the 1 wt.% solution the final thickness is almost similarly independent of the casting thickness, as presented in Table 1. It seems that the pores of the sheets cast at 1000 μm are compressed, leading to a reduced porosity in comparison to the sheets cast at 500 μm. For these sheets with relative weak morphology, the imprint of the micropattern is not preserved when casting on a patterned mold.

Table 1
Porosity of PLLA HMw sheets: np refers to the nonpatterned mold and 25 μm refers to the mold featuring 25 μm wide continuous channels.

Polymer concentration (wt.%)	Initial casting thickness (μm)	Mold pattern (μm)	Final thickness (average, μm)	Porosity (%)	Pattern replication
1	500	np	13 ± 0.3	68 ± 3	
		25	13 ± 0.8	64 ± 3	No
	1000	np	14 ± 0.8	45 ± 5	
		25	14 ± 0.7	50 ± 1	No
1.5	500	np	15 ± 0.1	65 ± 3	
		25	13 ± 1.5	61 ± 1	No
	1000	np	21 ± 0.9	52 ± 5	
		25	27 ± 2.0[a]	60 ± 1	Superficial
2	500	np	26 ± 1.7	75 ± 2	
		25	26 ± 0.5	71 ± 1	Superficial
	1000	np	35 ± 0.6	63 ± 1	
		25	80 ± 3.6	81 ± 1	Yes

[a] Locally macrovoid formation was observed for these sheets; value indicates the thickness of the continuous part of the sheet where no macrovoids were present (left side of the sheet in Fig. 2d).

A transition occurs for the sheets cast of the 1.5 wt.%. The sheets cast at 1000 μm are thicker and have a slightly reduced porosity compared to the sheets cast at 500 μm, see Table 1. Besides, the fiber morphology at the substrate surface appears denser in comparison to that cast from the 1 wt.% solution. The sheets cast on the patterned molds have an imprint of the channel pattern at the substrate side, but only on the surface with almost no channel depth. Interestingly, the sheets cast at 1000 μm on the micropatterned mold show local macrovoid formation as a result of fast inflow of the nonsolvent at the substrate side. Perhaps the channel pattern on the mold creates space for the nonsolvent to enter the polymer sheet at a higher rate as compared to the nonpatterned molds where all nonsolvent inflow is from the top and sides of the sheets.

The sheets cast of the 2 wt.% solution have a higher thickness and porosity compared to those cast of the 1 and 1.5 wt.% solutions (Table 1). In fact, in these sheets the diameter of the fibers is rather similar to those of the sheets produced of the 1 and 1.5 wt.% solutions, but the packing of the fibers appears to be less dense, yielding sheets with higher porosity. Sheets cast from the 2 wt.% solution at the patterned mold at a casting thickness of 500 μm show an imprint of the micropattern, similar to the sheets of the 1.5 wt.% solutions, as presented in Fig. 2a,b. Only for the sheets cast at 1000 μm do microchannels clearly imprint into the polymer sheets, indicating that these sheets have sufficient mechanical strength to maintain the micropattern during solidification of the polymer matrix (see Fig. 2c,d). However, these micropatterned sheets are not as highly fibrous but have more solid-wall-like pores although still with very high porosity of 81% and their surfaces have a certain level of nano-fibrous morphology, especially on the air side. This is an interesting result which shows the versatility of the method. Nonetheless, to obtain micropatterned scaffolds with more nano-fibrous morphology, one needs to optimize further the casting conditions, especially finding the optimal polymer concentration in combination to sheet casting thickness.

In conclusion, our results suggest that the nano-fibrous morphology of the HMw PLLA sheets is due to a very low polymer volume in combination with a sufficiently strong transient network as a result of the longer molecular chains. As mentioned before, for the control PLLA the polymer-rich phase cannot form the continuous matrix at such low polymer concentrations. Clearly, use of higher concentration of HMw PLLA solution leads to increased total

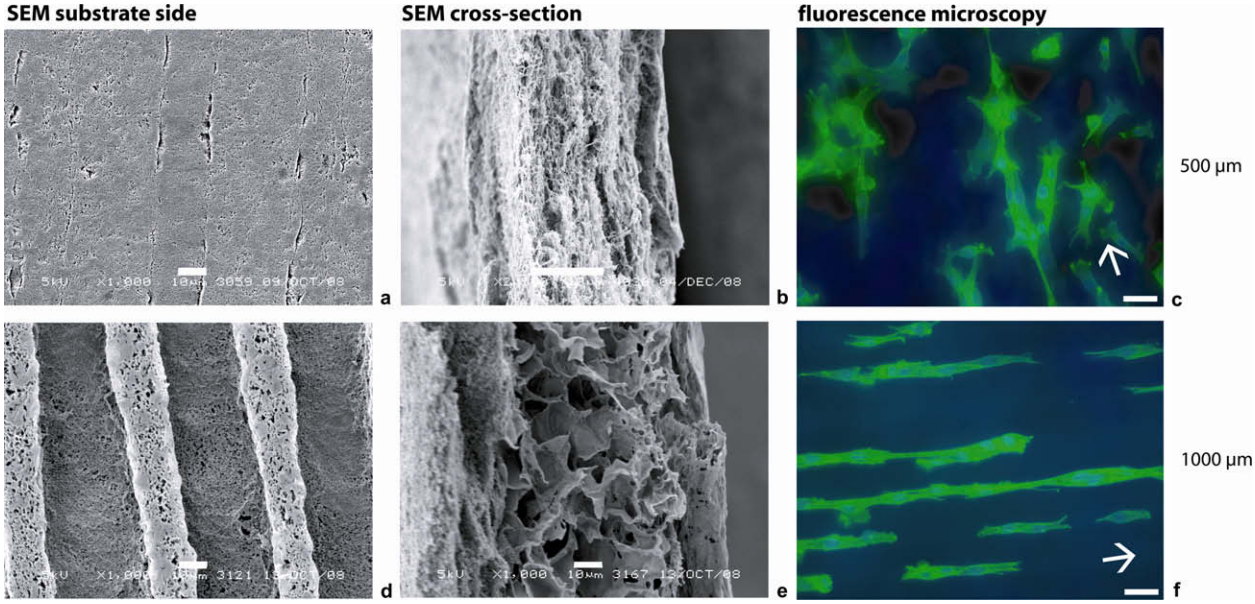

Fig. 2. Typical (a–b, d–e) SEM and (c, f) fluorescence microscopy images of sheets cast from a 2 wt.% PLLA HMw concentration solution on the mold featuring continuous 25 µm wide channels with initial casting thickness of (a–c) 500 µm and (c–f) 1000 µm; (c, f) C2C12 cells, seeding density 5000 cells cm^{-2} at day 3. Bar in images represents (a–b, d–e) 10 µm and (c, f) 25 µm. The arrows indicate channel direction.

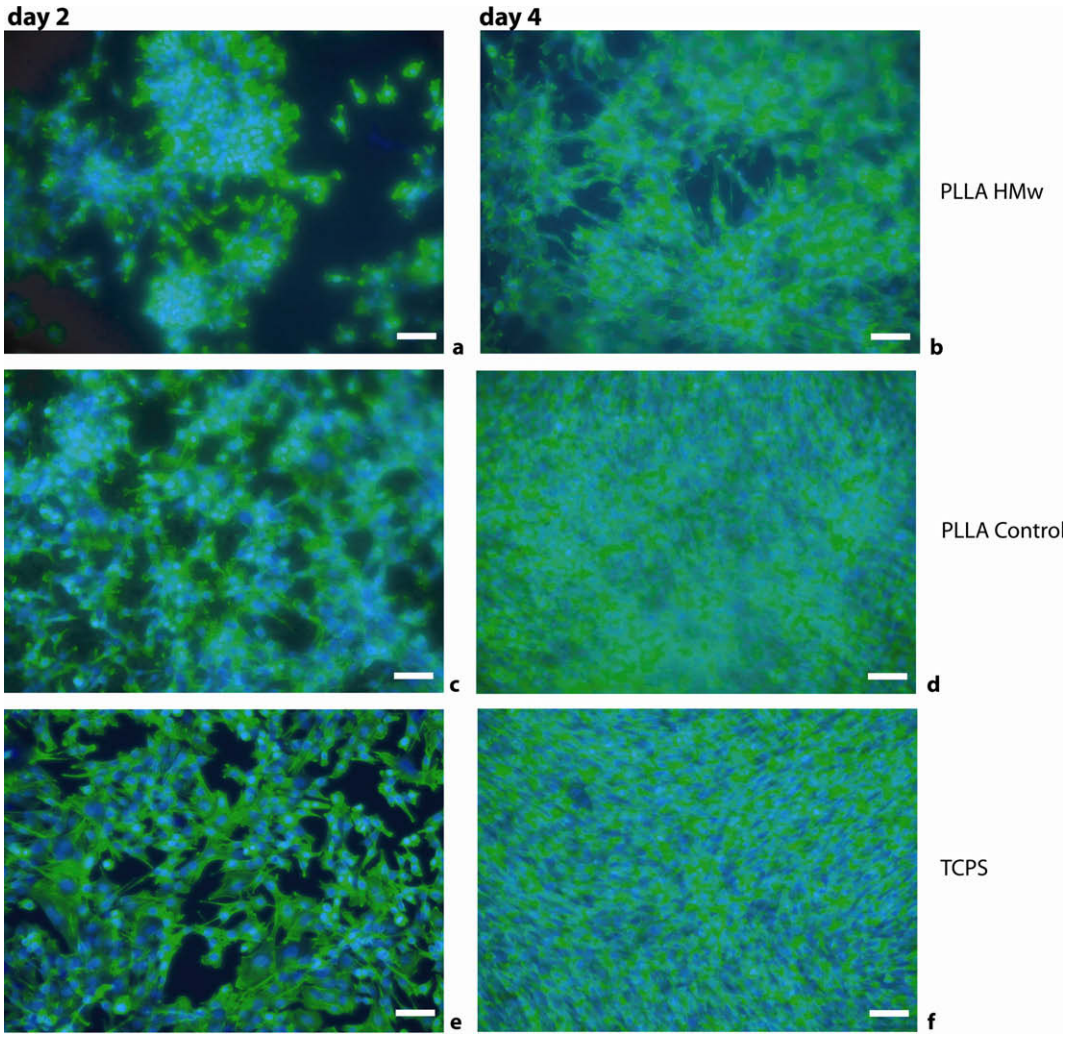

Fig. 3. Typical fluorescence microscopy images illustrating C2C12 cells growing on nonpatterned (a, b) PLLA HMw sheets cast from a 2 wt.% polymer concentration solution at initial casting thickness of 500 µm, (c, d) PLLA control sheets and (e, f) TCPS at (a, c, e) day 2 and (b, d, f) day 4. Seeding density 15,000 cells cm^{-2}, cells stained for cytoskeleton (green, AlexaFluor 488 phalloidin) and nuclei (blue, Hoechst), magnification 10×, scale bar in images represents 25 µm.

polymer volume, and thus results in a polymer sheet with bigger characteristics sizes and (partial) loss of nano-fibrous morphology.

3.5. Cell culture and analysis

Fig. 3 displays typical fluorescent microscopy images of stained cytoskeletons and nuclei of cultured pre-myoblasts, C2C12, on nonpatterned PLLA HMw (cast from a 2 wt.% solution at 500 μm initial casting thickness) and PLLA control sheets as well as tissue culture polystyrene (TCPS) as reference. Fig. 4 presents typical SEM images the C2C12 morphology on the PLLA HMw sheets. As indication for proliferation at different time points, Fig. 5 presents DNA concentration data of C2C12 cells on PLLA HMw and PLLA control sheets as well as TCPS as reference. Earlier experience with C2C12 cell culture on dense (non-porous) sheets prepared by both PLLA control and PLLA HMw showed no difference regarding C2C12 attachment, proliferation and morphology [30]. Therefore, we can assume that variation in cell behavior between the PLLA control and PLLA HMw sheets is only due to the difference in sheet morphology between the two cases.

The results reveal that the cells adhere and proliferate very well on the PLLA HMw sheets. In fact; the cell–cell contact between the cells on the PLLA HMw sheets seems to be better compared to the PLLA control sheets and TCPS (see also Ref. [30]). This observation is in agreement with the literature, where it was reported that in various cell types integrins associated with cell–cell as well as cell–ECM contact were up-regulated on nano-fibrous scaffolds compared to flat surfaces as a response to increase protein adsorption [15]. The SEM images in Fig. 4 support this observation as the C2C12 cells spread well on the PLLA HMw sheets and show good connection between the cells' filopodia as well as the cells with the nano-fibrous surface. The DNA assay data (Fig. 5) indicates slightly increased cell proliferation on the PLLA HMw sheets compared to the PLLA control sheets, although only significant at day 4 for the higher cell density.

Additionally, for the micropatterned sheets (2 wt.% solution cast at 1000 μm) the C2C12 cells align perfectly in the direction of the channels (see Fig. 2f). For the sheets cast at 500 μm, the cells also appear to align to a certain extent along the channels, even though the pattern is not prominently imprinted into the sheets (Fig. 2c). Topographical patterning with these dimensions is known to induce good alignment of C2C12 cells [3]. These results confirm that these cells adhere, spread and proliferate very well on the PLLA HMw surfaces with nano-fiber morphology and that excellent cell alignment can be reached using patterned sheets.

4. Conclusions

This work presents a facile method to fabricate highly porous PLLA scaffold sheets with nano-fibrous morphology. The sheets

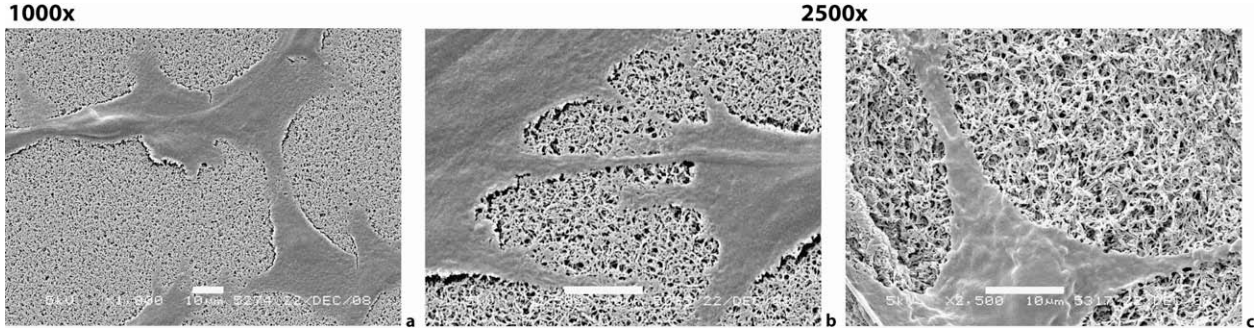

Fig. 4. Typical SEM images illustrating C2C12 cell growth on nonpatterned PLLA HMw sheets: (a) magnification 1000×, (b, c) magnification 2500×, bar in images represents 10 μm.

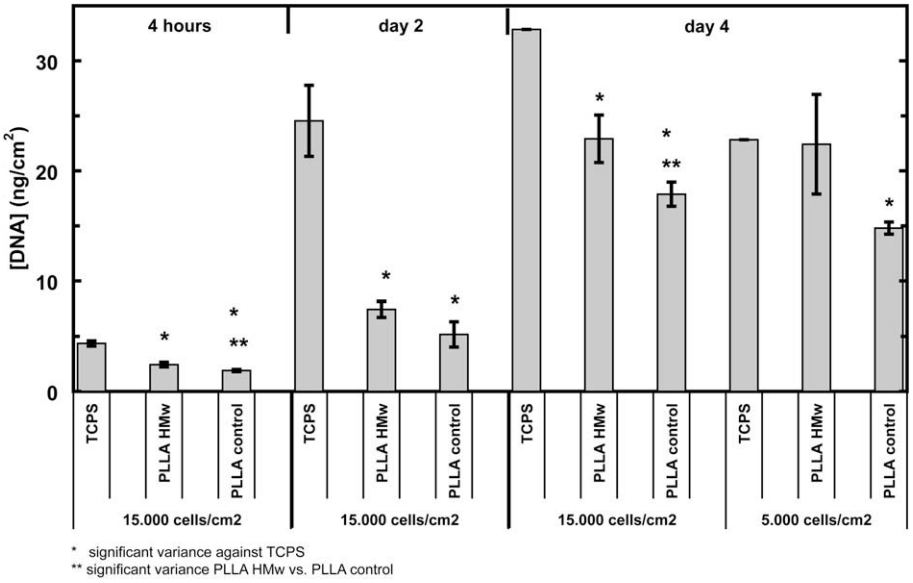

Fig. 5. DNA assay for nonpatterned PLLA HMw (cast from a 2 wt.% polymer concentration solution at initial casting thickness of 500 μm) and PLLA control sheets, and as reference TCPS, at after 4 h of attaching and at day 2 and 4. Seeding density of 5000 and 15,000 cells cm^{-2}, significance was calculated by a two-tailed *t*-test with $p < 0.05$, error bars indicate standard deviation.

were produced by phase inversion using very low polymer concentration solutions of very-high-molecular-weight PLLA (M_w of 5.72×10^5 g mol^{-1}). For the PLLA HMw, the critical polymer concentration for sheet formation is low, thus allowing the formation of highly interconnected porous sheets with nano-fibers within the range of 50–500 nm. Besides, PSμM enables micropatterning of these nano-fibrous sheets at optimized polymer concentrations. Culturing of C2C12 cells on these nano-fibrous sheets reveals good cell adhesion, spreading and proliferation; and in the case of imprinted microchannels, excellent alignment of the cells along the channels.

This study shows that PSμM is a facile method to produce micropatterned nano-fibrous PLLA sheets with morphologies comparable to those obtained by other more elaborate methods, such as electrospinning. These micropatterned nano-fibrous sheets will be further evaluated for tissue engineering applications. In fact, our future work will focus at constructing 3D scaffolds by stacking these nano-fibrous PLLA sheets (similar to our previous work performed for control PLLA sheets [3,31]). In our concept, the micropatterned channels allow nutrient supply to the cells and induce cell organization whereas the microporosity of the sheets allows nutrient transport throughout the scaffold and communication between the cell layers [31]. The degradation time of PLLA is relatively long (in the order of 12 months in vitro and 8–10 months in vivo), and the cells will build up their own ECM before the PLLA sheet would lose its ECM-like morphology. We therefore expect that the nano-fibrous PLLA scaffold will keep its superior characteristic to mimic ECM long enough to help produce good-quality tissue.

Acknowledgments

The authors would like to thank Dr. J. de Boer and Prof. Dr. C.A. van Blitterswijk (Department of Tissue Regeneration, University of Twente, The Netherlands) for facilitating the cell culture experiments. This project is financially supported by the Spearhead program: "Advanced Polymeric Microstructures for Tissue Engineering" of the University of Twente (MIRA, Institute for Biomedical Technology and Technical Medicine).

Appendix A. Figures with essential color discrimination

Certain figures in this article, particularly Figs. 2 and 3, are difficult to interpret in black and white. The full color images can be found in the on-line version, at doi:10.1016/j.actbio.2009.12.051.

References

[1] Ma PX. Scaffolds for tissue fabrication. Mater Today 2004;7:30.
[2] Yang S, Leong K-F, Du Z, Chua C-K. The design of scaffolds for use in tissue engineering. Part I. Traditional factors. Tissue Eng 2001;7:679.
[3] Papenburg BJ, Vogelaar L, Bolhuis-Versteeg LAM, Lammertink RGH, Stamatialis D, Wessling M. One-step fabrication of porous micropatterned scaffolds to control cell behavior. Biomaterials 2007;28:1998.
[4] Sawalha H, Schroën K, Boom R. Polylactide films formed by immersion precipitation: effects of additives, nonsolvent, and temperature. J Appl Polym Sci 2007;104:959.
[5] Tu C, Cai Q, Yang J, Wan Y, Bei J, Wang S. The fabrication and characterization of poly(lactic acid) scaffolds for tissue engineering by improved solid–liquid phase separation. Polym Adv Technol 2003;14:565.
[6] Zoppi RA, Contant S, Duek EAR, Marques FR, Wada MLF, Nunes SP. Porous poly(L-lactide) films obtained by immersion precipitation process: morphology, phase separation and culture of VERO cells. Polymer 1999;40:3275.
[7] Hua FJ, Kim GE, Lee JD, Son YK, Lee DS. Macroporous poly(L-lactide) scaffold 1. Preparation of a macroporous scaffold by liquid-liquid phase separation of a PLLA-dioxane-water system. J Biomed Mater Res 2002;63:161.
[8] Li S, Carrubba VL, Piccarolo S, Sannino D, Brucato V. Preparation and properties of poly(L-lactic acid) scaffolds by thermally induced phase separation from a ternary polymer-solvent system. Polym Int 2004;53:2079.
[9] Nam YS, Park TG. Porous biodegradable polymeric scaffolds prepared by thermally induced phase separation. J Biomed Mater Res 1999;47:8.
[10] Boudriot U, Dersch R, Greiner A, Wendorff JH. Electrospinning approaches toward scaffold engineering – a brief overview. Artif Organs 2006;30:785.
[11] Chen R, Hunt JA. Biomimetic materials processing for tissue-engineering processes. J Mater Chem 2007;17:3974.
[12] Ma Z, Ramakrishna S. Nanostructured extracellular matrix. Encycl Nanosci Nanotechnol 2004;7:641.
[13] Moroni L, De Wijn JR, Van Blitterswijk CA. Integrating novel technologies to fabricate smart scaffolds. J Biomater Sci Polym Ed 2008;19:543.
[14] Stevens MM, George JH. Exploring and engineering the cell surface interface. Science 2005;310:1135.
[15] Kumar C. Tissue, cell and organ engineering. Weinheim: Wiley-VCH Verlag GmbH & Co.; 2006.
[16] Bhattarai SR, Bhattarai N, Viswanathamurthi P, Yi HK, Hwang PH, Kim HY. Hydrophilic nanofibrous structure of polylactide; fabrication and cell affinity. J Biomed Mater Res A 2006;78A:247.
[17] Inai R, Kotaki M, Ramakrishna S. Structure and properties of electrospun PLLA single nanofibres. Nanotechnology 2005;16:208.
[18] Moroni L, Licht R, de Boer J, de Wijn JR, van Blitterswijk CA. Fiber diameter and texture of electrospun PEOT/PBT scaffolds influence human mesenchymal stem cell proliferation and morphology, and the release of incorporated compounds. Biomaterials 2006;27:4911.
[19] Riboldi SA, Sampaolesi M, Neuenschwander P, Cossu G, Mantero S. Electrospun degradable polyesterurethane membranes: potential scaffolds for skeletal muscle tissue engineering. Biomaterials 2005;26:4606.
[20] Woo KM, Jun J-H, Chen VJ, Seo J, Baek J-H, Ryoo H-M, et al. Nano-fibrous scaffolding promotes osteoblast differentiation and biomineralization. Biomaterials 2007;28:335.
[21] Yang F, Murugan R, Ramakrishna S, Wang X, Ma YX, Wang S. Fabrication of nano-structured porous PLLA scaffold intended for nerve tissue engineering. Biomaterials 2004;25:1891.
[22] Park H, Cannizzaro C, Vunjak-Novakovic G, Langer R, Vacanti CA, Farokhzad OC. Nanofabrication and microfabrication of functional materials for tissue engineering. Tissue Eng 2007;13:1867.
[23] De Gennes PG, editor. Scaling concepts in polymer science. Oxford: Oxford University Press; 1979.
[24] Graessley WW, Edwards SF. Entanglement interactions in polymers and the chain contour concentration. Polymer 1981;22:1329.
[25] Osaki K, Nishizawa K, Kurata M. Material time constant characterizing the nonlinear viscoelasticity of entangled polymeric systems. Macromolecules 1982;15:1068.
[26] Rubinstein M, Helfand E. Statistics of the entanglement of polymers: concentration effects. J Chem Phys 1985;82:2477.
[27] Prevorsek DC, De Bona BT. On chain entanglement in high-T_g amorphous polymers. II, vol. 25. London: Taylor & Francis; 1986. p. 515.
[28] Porter RS, Johnson JF. The entanglement concept in polymer systems. Chem Rev 1966;66:1.
[29] Pvd Witte, Dijkstra PJ, van den Berg JWA, Feijen J. Phase separation processes in polymer solutions in relation to membrane formation. J Membr Sci 1996;117:1.
[30] Papenburg BJ. Design strategies for tissue engineering scaffolds. Ph.D. thesis. University of Twente, Enschede; 2009.
[31] Papenburg BJ, Liu J, Higuera GA, Barradas AMC, de Boer J, van Blitterswijk CA, et al. Development and analysis of multi-layer scaffolds for tissue engineering. Biomaterials 2009;30:6228.